

High activity of He droplets following ionization of systems inside those droplets

Nikolai V. Kryzhevoi,* Vitali Averbukh, and Lorenz S. Cederbaum

Theoretical Chemistry, Institute of Physical Chemistry at Heidelberg University,

Im Neuenheimer Feld 229, 69120 Heidelberg, Germany

(Dated: August 5, 2018)

Abstract

Relaxation processes following *inner-valence* ionization of a system can be modified dramatically by embedding this system in a suitable environment. Surprisingly, such an environment can be even composed of helium atoms, the most inert species available. As demonstrated by the examples of Ne and Ca atoms embedded in He droplets, a fast relaxation process [Interatomic Coulombic Decay (ICD)] takes place merely due to the presence of the He surroundings. We have computed ICD widths for both $^4\text{He}_N$ and $^3\text{He}_N$ droplets doped with Ne and Ca and discuss the findings in some detail. In the case of Ne, ICD is by far the dominating relaxation pathway. In Ca, atomic Auger decay is also possible but ICD becomes a competitive relaxation pathway in the droplets.

PACS numbers: 67.40.Fd, 67.40.Yv, 31.70.Dk, 36.40.Mr

*e-mail: nikolai.kryzhevoi@pci.uni-heidelberg.de

Helium droplets have been attracting considerable attention due to their unique properties. We refer the reader to review papers describing the present state of the art of the field of helium droplets, its profound achievements and open questions [1, 2]. The broad interest in He droplets derives from the recognition that they can easily pick up foreign species. Numerous experimental and theoretical studies pursued several objectives such as to gain a better insight into the properties of the pure He drops themselves as well as to derive valuable information on dopants, taking advantage of the He droplets as an ultracold and gentle matrix in high resolution spectroscopies.

Because of the weak impurity-helium interaction, properties of the impurity are usually little affected by the He surroundings. However, even minor changes, e.g. small shifts of various transitions of a foreign atom due to embedding in a He droplet, are of crucial importance since they can shed additional light on the nature of the impurity-helium interaction and are very helpful, for example, in predicting the impurity position in the droplet[3, 4, 5]. Cases where the He environment modifies markedly the properties of a system embedded in a He droplet attract special attention. To our knowledge only a few such cases have been reported so far, notably in all of them the droplets were subject to ionization[6, 7].

Irradiation of doped droplets with femtosecond laser pulses causes a rich palette of charged ions as a result of droplet disintegration via Coulomb explosion. Although singly charged He atoms appear as well[8, 9] the cause for their appearance did not receive the attention it deserves. One possibility of the He ions production is obviously the direct ionization by intense laser pulses. Another way one might think of is much more exciting since it reveals a high activity of the He environment in processes occurring in doped He droplets. Here, the He ions are the outcome of a very efficient relaxation pathway of highly excited states of the *foreign* systems embedded in the droplets which is operative *only* due to the presence of the He environment. This relaxation process is Interatomic Coulombic Decay (ICD) [10, 11, 12, 13, 14, 15, 16].

Generally, relaxation of an inner-valence vacancy in an isolated atom proceeds radiatively by emission of a photon, in contrast to a deeper core vacancy which decays by ejecting an Auger electron. The situation can change drastically if neighboring atoms are present as predicted theoretically[10] and confirmed experimentally[11, 12]. The presence of a neighboring atom lowers the double ionization threshold of the system compared to that of the isolated atom. If this threshold is now below the energy of the inner-valence hole state, a novel radia-

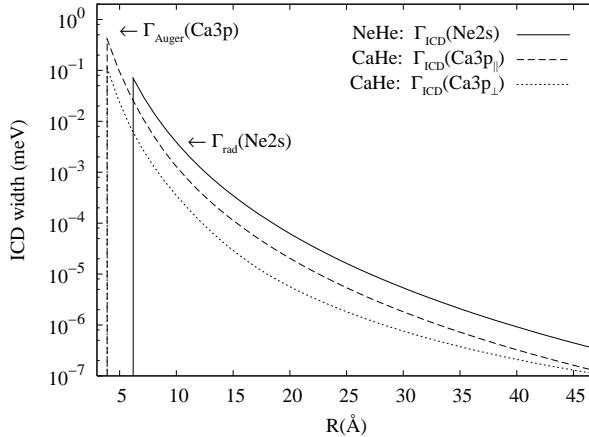


FIG. 1: ICD widths of inner-valence vacancies in the NeHe and CaHe pairs as functions of the interatomic distance. The $\text{Ca}3p_{\parallel}$ and $\text{Ca}3p_{\perp}$ orbitals are parallel and perpendicular to the Ca–He axis. The widths of the dominant decay processes in the isolated Ne and Ca atoms are labeled.

tionless decay channel opens. In the ICD process the initial inner-valence vacancy is filled by an outer-valence electron from the same atomic site while the energy released is transferred to ionize a *neighboring* subunit of the system. ICD may have dramatic consequences for a system where it takes place making this system unstable towards fragmentation due to the occurrence of two spatially separated charges.

ICD is an *interatomic* process in its nature and this makes its properties, in particular the decay width Γ_{ICD} or equivalently the lifetime τ_{ICD} of the inner-valence hole, strongly environment dependent. In the classical example of the $2s$ ionization of a Ne atom, the $2p \rightarrow 2s$ relaxation energy of 26.91 eV is insufficient for emitting another electron from this atom. The $\text{Ne}2s$ hole decays, therefore, radiatively in about 175 ps [17] corresponding to Γ_{rad} of 3.8 μeV . On the other hand, if a neighboring Ne atom is present, the 26.91 eV are sufficient to knock a $2p$ electron out of this neighboring Ne atom and to make ICD operative [12, 13]. In the Ne dimer τ_{ICD} is about 85 fs, more than 2000 times smaller than τ_{rad} ! The lifetime of the $\text{Ne}2s$ vacancy reduces further to only a few femtoseconds if the excited Ne atom is surrounded by several neighbors like it is the case in a Ne_N cluster [14, 15].

Interestingly, the above mentioned energy of 26.91 eV is also sufficient to ionize a neighboring He atom. For this to occur, the minimal separation between He and Ne should be $R_{\text{ICD}} = 6.2 \text{ \AA}$ which is derived under the plausible assumption that the ionization energy of He in the presence of the Ne ion is governed by electrostatic repulsion between both. Is the

presence of a by far more distant He atom which is less perturbing than Ne able to modify considerably the decay of the Ne2s vacancy like it happens in Ne₂? To answer this question we have calculated $\Gamma_{\text{ICD}}^{\text{pair}}(R)$ for a pair of Ne and He separated by $R \geq R_{\text{ICD}}$ using a recently developed *ab initio* Fano-GF method[16]. The method represents a combination of a Fano formalism for resonance widths, a Green's Function method for solving a multielectron problem, and a Stieltjes imaging technique for renormalization of the discretized continuum (see Ref. [16] for details). Together with the d-aug-cc-pVQZ basis sets for Ne and He [18] we used continuum-like diffuse functions of *s*, *p* and *d* types[19] distributed between these atoms as well as around He. The results are shown by the solid curve in Fig. 1. The dominance of ICD over radiative decay at R_{ICD} ($\Gamma_{\text{ICD}}^{\text{pair}} = 70\mu\text{eV}$) and some larger R is apparent. This fact, being striking by itself, is however of minor consequence for the diatomic NeHe cluster since the probability to find Ne and He at such large separations (more than twice the equilibrium distance of the cluster) is negligible despite the floppiness of this system.

Being captured by a He droplet, Ne can be surrounded by tens, hundreds or even thousands He atoms, many of them residing at sufficiently large distances from the impurity to make ICD of the Ne2s vacancy possible. Since the ICD performance increases with opening new ICD channels, ICD is expected to be more and more pronounced as the droplet size grows. The big size of a droplet is a serious obstacle for calculating ICD widths from first principles. Intuition suggests however that the interaction of a dopant with a He atom is not strongly perturbed by other He atoms so that $\Gamma_{\text{ICD}}^{\text{drop}}$ for doped droplets can be reliably approximated by a sum of $\Gamma_{\text{ICD}}^{\text{pair}}$ for individual dopant-He pairs. The *ab initio* calculations below support this view.

Using the Fano-GF method we have explicitly calculated $\Gamma_{\text{ICD}}^{\text{clust}}$ for the most symmetric NeHe_{*N*} ($N=1-4$) clusters with Ne in the center. The He atoms were separated from Ne by 6.4 Å, a typical radius of the second coordination shell in He droplets doped with Ne (the first coordination shell is ICD-inactive). To keep the size of the problem tractable for the *ab initio* method used, we had to reduce the quality of the basis set for He to d-aug-cc-pVTZ. Excellent agreement between the results obtained and those derived by multiplication of $\Gamma_{\text{ICD}}^{\text{pair}}$ with N (see Fig. 2) strongly suggests the validity of the pairwise additivity of ICD widths. Other clusters have also been studied leading to the same conclusions (see below).

Assuming pairwise additivity also in larger systems, we can now estimate $\Gamma_{\text{ICD}}^{\text{drop}}$ for Ne@He_{*N*} droplets. Ne is known to locate in the center of both ⁴He and ³He droplets

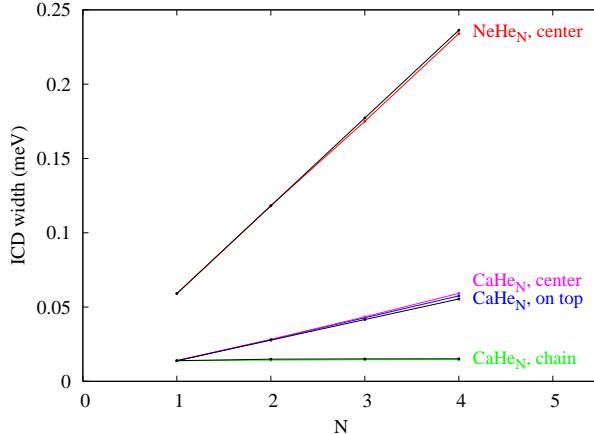


FIG. 2: (Color online). Comparison of the explicitly *ab initio* calculated ICD widths (color lines) with those obtained using the pairwise additivity approximation (black lines). Some nearby curves are hardly distinguishable.

[20, 21] as a consequence of a stronger Ne–He interaction compared to the He–He one. The density distribution ρ of helium around Ne is spherically symmetric and we may write $\Gamma_{\text{ICD}}^{\text{drop}} = 4\pi \int_{R_0}^{\infty} \Gamma_{\text{ICD}}^{\text{pair}}(r)\rho(r)r^2 dr$, where R_0 is a cutoff radius below which the He atoms in the droplets are ICD-inactive. Due to the combined effect of the He environment, R_0 differs slightly from R_{ICD} . To assess R_0 , we have calculated ionization thresholds in different NeHe_N clusters, the largest one contains 18 He atoms distributed in two shells around the central Ne. The double (Ne2*p*–He1*s*) and Ne2*s* ionization thresholds of these systems were found to be lower than their counterparts in NeHe by up to 0.1 and 0.2 eV, respectively, which results in $R_0 = 5.93\text{\AA}$. These changes are consistent with the experimentally detected ones of ionization thresholds of He[22] and impurities[23] in larger He droplets supporting our results used to determine the cutoff radius R_0 in doped Ne@He_N droplets.

We have estimated $\Gamma_{\text{ICD}}^{\text{drop}}$ for several Ne@⁴He_N and Ne@³He_N droplets (in Fig. 3, circles joined by red and blue lines, respectively) with 50 to 5000 He atoms using actual density profiles of the doped droplets ρ_{dop} (filled circles) wherever possible and density profiles of the pure droplets ρ_{pure} (open circles) otherwise. All density profiles mentioned here and further on have been obtained by Barranco and co-workers within density functional theory (see Refs.[21, 24] for details). Whenever ρ_{pure} had to be used (note that this is only the case for ³He_N) we considered R_0 as a parameter serving to compensate for using the improper density distribution. Once obtained in the case where both ρ_{dop} and ρ_{pure} were available, the new R_0 was then applied for all droplets with unknown ρ_{dop} . $\Gamma_{\text{ICD}}^{\text{drop}}$ exhibits similar behaviors

with N for both doped ${}^4\text{He}_N$ and ${}^3\text{He}_N$ droplets. It rises rapidly for small N approaching a saturation limit of 1.8 meV ($\tau_{\text{ICD}}=360$ fs) and 1.4 meV ($\tau_{\text{ICD}}=480$ fs) at $N \sim 1000$ in the doped ${}^4\text{He}_N$ and ${}^3\text{He}_N$ droplets, respectively. Astonishingly, such drastic reductions of the Ne2s vacancy lifetime to a sub-picosecond timescale compared to that in the isolated Ne become possible due to the presence and with the active involvement of the He environment, the most inert environment available.

The spectacular ability of He environment to modify dramatically the course of processes occurring in highly excited species embedded in this environment is obviously not restricted to Ne. Another interesting example is provided by doped Ca@He $_N$ droplets. In contrast to the Ne2s vacancy, the Ca3p vacancy in an isolated Ca atom can undergo Auger decay. The $4s \rightarrow 3p$ relaxation energy of 28.31 eV is more than sufficient for autoionizing an outer-valence Ca4s electron resulting in Ca $^{2+}4s^{-2}$. This decay is characterized by a width of 0.58 meV according to our *ab initio* calculation using the Fano-GF method. Radiative decay of the Ca3p vacancy is much less efficient. The energy of 28.31 eV is high enough for ionizing a neighboring He atom via the ICD mechanism. Irrespective of the direction of the Ca3p orbital, the ICD widths in a CaHe pair for all Ca–He separations except for irrelevant short ones are noticeably exceeded by Γ_{Auger} (see Fig. 1).

What happens when Ca is ionized in a He droplet? Auger decay is inherently an *intra-atomic* process and its properties are only weakly influenced by the very inert He environment. By contrast, ICD is an *interatomic* process in character and its efficiency grows with additional He atoms attached. Thereby, not only the distances from Ca to individual He atoms play a crucial role, but also the orientation of the Ca3p $_i$ ($i = x, y, z$) orbital. Apparently, at a given distance the He atoms along the direction of a particular Ca3p $_i$ orbital contribute most to the corresponding ICD width $\Gamma_{i\text{ICD}}^{\text{drop}}$.

Ca is a remarkable element as far as its interaction with He droplets is concerned. Being picked up by a ${}^4\text{He}$ droplet Ca neither resides in the center nor is attached to surface of the droplet. It occupies an intermediate position in a quite deep surface dimple[5, 25]. In contrast to this, Ca sits in the center of a ${}^3\text{He}$ droplet as predicted recently[26]. The various $\Gamma_{i\text{ICD}}^{\text{drop}}$ are equal in Ca@ ${}^3\text{He}_N$ given that the ${}^3\text{He}$ distribution is isotropic, and slightly different in Ca@ ${}^4\text{He}_N$ because the ${}^4\text{He}$ distribution is not very anisotropic in the close vicinity of Ca residing in a deep dimple.

Variation of the average ICD width $\bar{\Gamma}_{\text{ICD}}^{\text{drop}} = 1/3 \sum \Gamma_{i\text{ICD}}^{\text{drop}}$ with droplet size is of larger

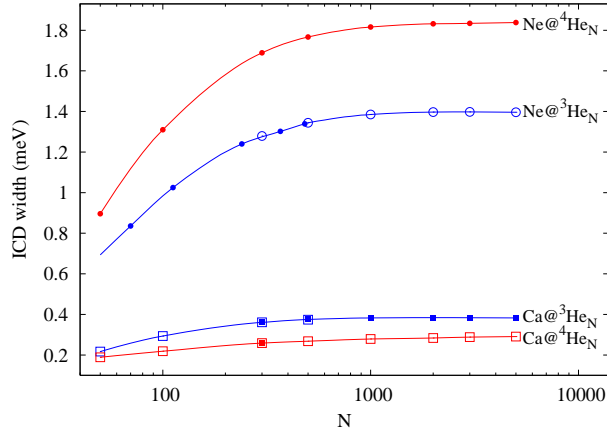


FIG. 3: (Color online). Estimated ICD widths of inner-valence vacancies in Ne and Ca doped in ^4He and ^3He droplets of different size. Results obtained by using density profiles of doped and pure He droplets are labeled by filled and open symbols, respectively (see text for details).

practical significance than those of the individual $\Gamma_{i\text{ICD}}^{\text{drop}}$. To get insight how $\bar{\Gamma}_{\text{ICD}}^{\text{drop}}$ changes with the number of He atoms let us first consider three sets of small CaHe_N ($N = 1-4$) clusters with distinct He arrangements. In the first case Ca is placed 6 \AA apart from the end of a linear He_N chain with link size of 3.2 \AA . These distances are the typical radius of the first coordination shell and the separation between two coordination shells in He droplets doped with Ca, respectively. Our *ab initio* calculations show that all $\Gamma_{i\text{ICD}}^{\text{clust}}$ and thus $\bar{\Gamma}_{\text{ICD}}^{\text{clust}}$ fulfil pairwise additivity, i.e. in each cluster all explicitly calculated $\Gamma_{i\text{ICD}}^{\text{clust}}$ are well reproduced by the sums of ICD widths corresponding to the available different CaHe pairs (see lower part of Fig. 2 for $\bar{\Gamma}_{\text{ICD}}^{\text{clust}}$).

In the other two sets of examples we put the Ca-He separation to 6 \AA and arrange helium in such ways to mimic solvated and surface locations of Ca. In one case Ca is surrounded by He atoms to form a complex of the highest possible symmetry, in the other one Ca is placed on top of the planar, symmetric He_N subcluster with a characteristic He-He separation of 3.2 \AA . The following conclusions can be drawn from our calculations. Although $\Gamma_{i\text{ICD}}^{\text{clust}}$ (not shown) are very sensitive to the arrangement of the He atoms, $\bar{\Gamma}_{\text{ICD}}^{\text{clust}}$ depend only weakly on the He distribution. The calculated $\bar{\Gamma}_{\text{ICD}}^{\text{clust}}$ are shown in the middle part of Fig. 2 together with the $N \times \bar{\Gamma}_{\text{ICD}}^{\text{pair}}$ values expected when using pairwise additivity. In both sets of examples the variations of $\bar{\Gamma}_{\text{ICD}}^{\text{clust}}$ with N can be well approximated by straight lines whose slopes differ only slightly ($\approx 5\%$) from the lines $N \times \bar{\Gamma}_{\text{ICD}}^{\text{pair}}$.

The above findings are of great help for estimating $\bar{\Gamma}_{\text{ICD}}^{\text{drop}}$ for large droplets since the numbers of ICD-active He atoms at each impurity–helium separation are the only quantities which count. For the case of an axial symmetric ^4He distribution exhibited in $\text{Ca}@^4\text{He}_N$ droplets we can write $\bar{\Gamma}_{\text{ICD}}^{\text{drop}} = 2\pi \int_{R_0}^{\infty} \bar{\Gamma}_{\text{ICD}}^{\text{pair}}(r) r^2 \int_0^\pi \rho(r, \vartheta) \sin \vartheta d\vartheta dr$, where ϑ is the angle between the radius-vector and a line joining the impurity position with the droplet center. $\bar{\Gamma}_{\text{ICD}}^{\text{drop}}$ for $\text{Ca}@^3\text{He}_N$ droplets which are characterized by a spherically symmetric ^3He distribution can be estimated according to the expression given above for $\text{Ne}@^4\text{He}_N$. Whenever ρ_{dop} is used we set the cutoff radius R_0 to 3.83 \AA corresponding to the distance in the diatomic CaHe at which ICD starts to operate. Although the actual R_0 in droplets is likely to be slightly different from this value, there is no need to know it precisely because He atoms are hardly present at such small separations from the impurity ($\rho_{\text{dop}} \approx 0.01\rho_{\text{bulk}}$ for $r \sim 4.5\text{\AA}$ [25, 26], where ρ_{bulk} is the bulk liquid He density).

The estimated $\bar{\Gamma}_{\text{ICD}}^{\text{drop}}$ for both $^3\text{He}_N$ and $^4\text{He}_N$ droplets doped with Ca are shown in Fig. 3 (squares joined by blue and red lines, respectively). The curves exhibit different behaviors with droplet size. While $\bar{\Gamma}_{\text{ICD}}^{\text{drop}}$ in the former case approaches a saturation limit of 0.38 meV ($\tau_{\text{ICD}}=1.7 \text{ ps}$) at $N \sim 800$, $\bar{\Gamma}_{\text{ICD}}^{\text{drop}}$ in the latter case has not saturated even at $N = 5000$. Moreover, it shows a clear tendency towards further increase for larger droplets indicating that the nearest surroundings of Ca (i.e. the dimple and its vicinity) is still under formation there. One sees that the ICD width in doped He droplets has grown markedly compared to that in CaHe . Although ICD has not become the dominant decay process in $\text{Ca}@^4\text{He}_N$ it has nevertheless become competitive with Auger decay due to the presence of the He environment.

In summary, unambiguous evidence of the ability of He droplets to modify significantly the course of ionization processes occurring in systems embedded in them has been furnished. It has been shown that the presence of a He environment enclosing Ne and Ca leads to Interatomic Coulombic Decay of their inner-valence vacancies. Other suitable dopants including atoms, molecules or clusters can undergo the same scenario as well. The pairwise additivity of the ICD width established in small clusters has allowed us to estimate the ICD widths in large droplets. The details of ICD depend noticeably on droplet size, droplet density and the dopant position and hence also on the He isotope of which the droplet is made. A comparison of the ICD performance with those of competitive relaxation mechanisms in the doped He droplets has revealed that ICD dominates by orders of magnitude

over radiative decay and matches the performance of Auger decay if the latter is possible. Note that ICD might have severe consequences for doped He droplets. The interaction of the He environment with the slow electrons and ions produced due to ICD can lead to changes of the structure or even to fragmentation of the droplets and are issues which merit further theoretical and experimental studies.

We express our gratitude to M. Barranco and his co-workers for valuable discussions and for providing us with the He density distributions for the pure and doped He droplets. Financial support by the DFG is gratefully acknowledged.

-
- [1] M. Barranco *et al.*, *J. Low Temp. Phys.* **142**, 1 (2006).
 - [2] F. Stienkemeier and K. K. Lehmann, *J. Phys. B* **39**, R127 (2006).
 - [3] F. Stienkemeier *et al.*, *Phys. Rev. B* **70**, 214509 (2004).
 - [4] J. Reho *et al.*, *J. Chem. Phys.* **112**, 8409 (2000).
 - [5] F. Stienkemeier *et al.*, *J. Chem. Phys.* **107**, 10816 (1997);
 - [6] T. Ruchti *et al.*, *J. Chem. Phys.* **109**, 10679 (1998); B. E. Callicoatt *et al.*, *ibid.* **108**, 9371 (1998).
 - [7] T. Döppner *et al.*, *Eur. Phys. J. D* **24**, 157 (2003).
 - [8] T. Döppner *et al.*, *Phys. Rev. Lett.* **94**, 013401 (2005).
 - [9] E. M. Snyder *et al.*, *Phys. Rev. Lett.* **77**, 3347 (1996).
 - [10] L. S. Cederbaum *et al.*, *Phys. Rev. Lett.* **79**, 4778 (1997).
 - [11] S. Marburger *et al.*, *Phys. Rev. Lett.* **90**, 203401 (2003).
 - [12] T. Jahnke *et al.*, *Phys. Rev. Lett.* **93**, 163401 (2004).
 - [13] S. Scheit *et al.*, *J. Chem. Phys.* **121**, 8393 (2004).
 - [14] R. Santra *et al.*, *Phys. Rev. B* **64**, 245104 (2001).
 - [15] G. Öhrwall *et al.*, *Phys. Rev. Lett.* **93**, 173401 (2004).
 - [16] V. Averbukh and L. S. Cederbaum, *J. Chem. Phys.* **123**, 204107 (2005).
 - [17] D. C. Griffin *et al.*, *J. Phys. B* **34**, 4401 (2001).
 - [18] D. E. Woon and T. H. Dunning, Jr., *J. Chem. Phys.* **100**, 2975 (1994).
 - [19] K. Kaufmann *et al.*, *J. Phys. B* **22**, 2223 (1989).
 - [20] A. Scheidemann *et al.*, *Phys. Rev. Lett.* **64**, 1899 (1990).

- [21] F. Garcias *et al.*, J. Chem. Phys. **108**, 9102 (1998).
- [22] S. Denifl *et al.*, J. Chem. Phys. **124**, 054320 (2006).
- [23] E. Loginov *et al.*, Phys. Rev. Lett. **95**, 163401 (2005).
- [24] F. Dalfovo *et al.*, Phys. Rev. B **52**, 1193 (1995).
- [25] F. Ancilotto *et al.*, Phys. Rev. Lett. **91**, 105302 (2003).
- [26] A. Hernando *et al.*, J. Phys. Chem. A in press.